STATUS OF ENVIRONMENTALLY ASSISTED CRACKING STUDIES BY THE BASALT WASTE ISOLATION PROJECT

D. R. Duncan
Rockwell Hanford Operations
Richland, Washington 99352

L. A. James
Westinghouse Hanford Company
Richland, Washington 99352

S. G. Pitman
Pacific Northwest Laboratory
Richland, Washington 99352

ABSTRACT

The methodology for environmentally assisted cracking testing of condidate container materials for a nuclear waste repository in basalt is described, as well as test results to date. Results have shown no crack extension in fracture mechanics tests and a range of environmentally assisted cracking susceptibility from slow strain rate tests, in basalt groundwater environments.

INTRODUCTION

Waste packages for storage of high-level nuclear waste in a repository in basalt must provide substantially complete containment of the waste for 300 to 1,000 yr [1]. The Basalt Waste Isolation Project (BWIP) waste package design includes three major components: (1) the waste form, (2) a metallic container, and (3) basalt/clay packing material enveloping the container. The reference container material is currently cast A27 carbon steel, although a recommendation for the final choice of container material has not yet been made. For the waste package to meet its containment requirements, the container must be shown to resist breach by any probable corrosion mode for its design lifetime of 300 to 1,000 yr. Environmentally assisted cracking (EAC), defined as cracking of a material by simultaneous action of an aggressive media and a tensile stress, is one of the possible corrosion modes. Within this report EAC will be used to mean both stress corrosion cracking and hydrogen embrittlement; usually these two types of EAC are discussed separately. Stress corrosion is an anodic process resulting from attack by some aggressive anion (such as chloride), while hydrogen embrittlement is a cathodic process caused by hydrogen. Both require the presence of a tensile stress, the aggressive ion, and a material susceptible to the cracking process. Either type of EAC might be possible in a repository in basalt from the groundwater anion content or the hydrogen that will be available from hydrolysis, radiolysis, or from corrosion of iron if a steel container is selected.

Testing and analysis of candidate container materials must be performed in the entire range of prototypic conditions expected in a repository in basalt to ascertain if EAC will occur.

There are four candidate container materials in the BWIP Container Materials Test Program.

- A27 grade 60-30 carbon steel
- A387 grade 9 low alloy steel (9 Cr - 1 Mo)
- Oxygen-free high conductivity (OFHC) copper (UNS C10200)
- Cupronickel 90-10 (UNS C70600).

The basalt groundwater is not expected to be strongly aggressive as far as EAC degradation. The groundwater from the current reference basalt flow (Grande Ronde Basalt, Cohassett flow) is a dilute solution of ~840 parts per million (p/m) dissolved solids. The solids are primarily sodium chloride with secondary constituents of bicarbonate, sulfate, silica, fluoride, potassium, and calcium. The pH of the groundwater is ~9.7. Details of the groundwater composition are given in Table I. The groundwater redox conditions are expected to be reducing, with very low dissolved oxygen content [2]. Other dissolved gases will include methane, nitrogen, argon, and carbon dioxide, with methane as the major component. Methane will be present at a concentration of 350 to 700 mg/L at prevailing temperature and pressure in the repository basalt strata. The preceding description is for equilibrium conditions reached after waste emplacement. Following emplacement of a waste container, there will be a period of time when its environment will be a vapor phase with some oxygen remaining from the construction and operation of the repository. The repository will then resaturate with groundwater and return to equilibrium conditions.

TABLE I

Composition of Actual and Synthetic Grande Ronde 4 Groundwater Solution.

Element	mg/L	Element	mg/L
Na^{+}	334	SO_4^{-2}	4.0
K^{+}	13.8	Si	45.0
Ca^{+2}	2.2	Inorganic carbon	18.1
F^{-}	19.9	pH	9.7
Cl^{-}	405		

Steels can be susceptible to EAC in nitrate, carbonate, or caustic environments or environments that provide readily available atomic hydrogen (such as hydrogen sulfide). The concentrations of these species are expected to be so dilute that the groundwater will be weakly aggressive at worst. The copper alloys are not expected to be susceptible to EAC in the groundwater, but there may be a potential for attack in the vapor environment if nitric acid is formed in a high enough concentration. This is not likely to occur as radiolysis at the container exterior will be too low with the current design of 8.5-cm wall thickness.

Prediction of EAC behavior in a quantitative manner can be elusive. If the environment is weakly aggressive, long and unpredictable time periods for initiation of cracking can result. Thus, formulating test programs and predicting long-term behavior from laboratory test results is challenging.

The BWIP test program for investigation of EAC behavior has two general types of testing, slow strain rate and fracture mechanics. The slow strain-rate tests use constant tensile extension rates on a smooth specimen in an environment of interest. The tests are conservative compared to expected service conditions. Slow strain-rate tests are used by BWIP as qualitative scoping and screening tools to rank candidate container alloy susceptibility and obtain information quickly. Fracture mechanics testing is employed to provide a basis for quantitative assessment of EAC susceptibility. The use of fracture mechanics has been confirmed by the National Academy of Sciences as the best available method of dealing with EAC problems [3]. Fracture mechanics specimens contain cracks part way through each specimen. Propagation of the crack with time is measured upon application of stress in an inert reference environment and in a simulated repository environment. Enhanced crack growth in the simulated repository environment would indicate EAC.

Two types of fracture mechanics tests are employed by BWIP, static load and cyclic load. Static load tests use a constant crack-mouth opening displacement for varying lengths of time. Cyclic load tests use loads varying with a constant repeating pattern; the frequency of each load cycle and the magnitude of maximum and minimum loads can be varied and adjusted to ensure measurable crack growth. Cyclic loading will not be encountered in an actual repository, but cyclic tests can provide a quantitative basis for conservative prediction of EAC behavior by calculation of a stress intensity (stress modified for effects of flaw geometry) threshold below which EAC would not occur for very long exposure times. If service stress intensities can be shown to be below this threshold, failure is theoretically impossible. This concept is illustrated in Fig. 1 and 2. The variation of the threshold stress intensity factor on applied stress and crack size is illustrated schematically in Fig. 1. A region with relatively low stress and low crack size will be free from EAC. Cyclic loading will decrease the threshold. Obtaining a stress intensity threshold from the fracture mechanics test results is shown in Fig. 2. Enough crack growth rate/stress intensity factor data would be obtained to make a defensible extrapolation down to a value assumed to represent a threshold. An extrapolation will be required because crack growth rates too slow to measure practically are still fast enough to penetrate a container wall in 300 to 1,000 yr.

A more complete description of the BWIP program for studying EAC is given in [4].

EXPERIMENTAL PROCEDURE

Slow Strain Rate

The slow strain-rate tests were performed using a refreshed autoclave system with a gear-driven mechanical loading device. Groundwater simulating the expected composition from the basalt strata proposed for the repository was pumped to the autoclave at 9 to 35 mL/h. The groundwater was

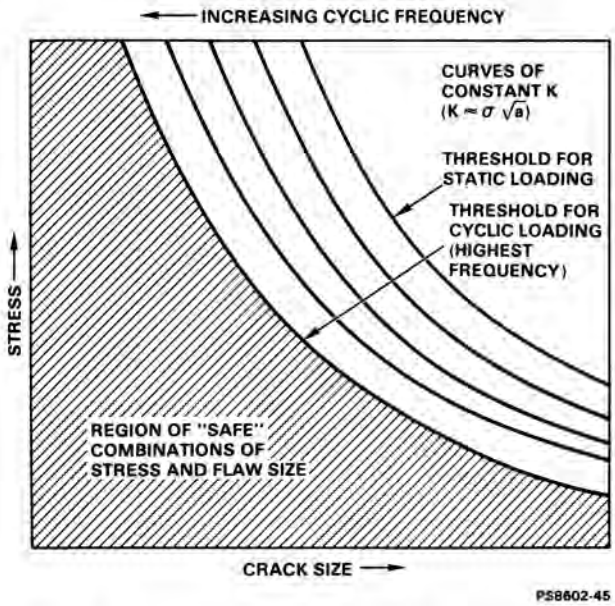

Fig. 1. Schematic Relationship Between Applied Stress, Crack Size, and Threshold Stress Intensity Factor.

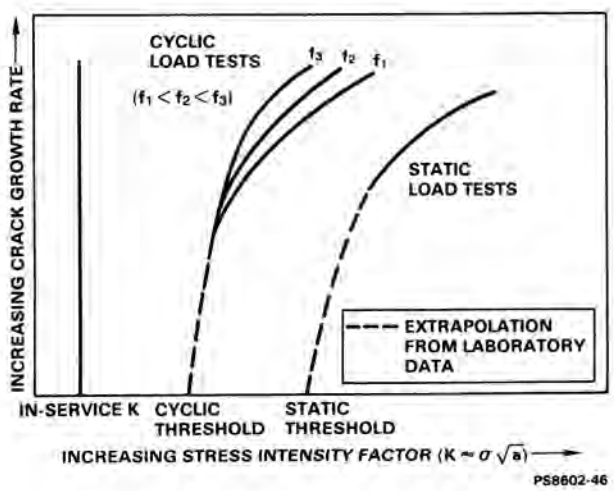

Fig. 2. Threshold Stress Intensity Factor and Fracture Mechanics Data.

pumped from a reservoir where it was sparged with argon or a mixture of argon and 20% oxygen. The inlet water flowed through a bed of crushed basalt before contacting the specimen. The dissolved oxygen content of the inlet water was ~8 p/m when sparged with argon and oxygen and less than 0.1 p/m

when sparged with argon. Tests of dissolved oxygen content of outlet water from the autoclave showed oxygen content less than 0.1 p/m for both sparging gases, demonstrating the reducing effect of the crushed basalt. Slow strain-rate tests were also conducted in air. Test temperatures were 100, 150, and 200 °C. No induced potentials were employed during the slow strain-rate tests, and the specimens were electrically isolated from the loading system.

Specimens were strained to failure at rates of 1×10^{-4}/s, 1×10^{-6}/s, and 2×10^{-7}/s. Yield and ultimate strengths were calculated from the load and displacement measurements. The elastic limit was taken as the yield strength rather than a 0.2% offset value due to limited resolution of the displacement measurements. Elongation and reduction of area values were taken from measurements of the failed specimens. Fractured specimens were cleaned in an inhibited acid solution and examined macroscopically for cracking or pitting. Selected specimens were examined with a scanning electron microscope to determine fracture mode and surface characteristics.

All of the BWIP candidate container materials have been examined with the slow strain-rate technique. Carbon steel has been tested in wrought and cast forms; the reference material now is the cast form. Compositions of the materials are given in Table II. The wrought 1020 steel was hot rolled. Two types of 1020 specimens were tested. The "LT" specimens were fabricated so that the test stress would be parallel to the plate rolling direction, while the "TL" specimens had testing stress perpendicular to the rolling direction. The yield point of the "TL" specimens was 286 MPa at room temperature, with an ultimate strength of 401 MPa. The "LT" specimens had a yield point of 263 MPa and an ultimate strength of 401 MPa at room temperature. The A27 (grade 60-30) steel was in an as-cast condition. The room temperature mechanical properties of the A27 material were a 0.2% yield strength of 352 MPa and an ultimate strength of 612 MPa. The A387-9 low-alloy steel was normalized at 900 °C for 52 min, air cooled, and then tempered at 720 °C for 61 min. The yield strength at room temperature of the A387 steel was 539 MPa and the ultimate strength was 683 MPa. The 90-10 Cupronickel alloy was annealed to a "soft" temper while the OFHC copper was a wrought, "half-hard" temper. The 0.5% yield point of the Cupronickel at room temperature was 129 MPa while the ultimate strength at room temperature was 279 MPa. Room temperature mechanical properties of the OFHC copper were not available but the room temperature hardness was 80.6 on the Rockwell "F" scale. Future tests of copper alloys will be in a fully annealed or cast condition as it is expected that the waste containers will be cast.

The Grande Ronde 2 groundwater composition used for most of the earlier experiments on 1020, A27, and A387 steels is given in Table III. Later tests used the Grande Ronde 4 groundwater composition given in Table I, which is the current reference composition. The Grande Ronde 4 composition is based on samples of groundwater from the Cohassett flow, the reference location for the repository. The two compositions are similar, dilute aqueous solutions and are expected to result in similar behavior in slow strain-rate tests.

Fracture Mechanics

Static load tests were performed with specimens of the modified-wedge/open-load (MWOL) design [5]. The MWOL specimens were pre-cracked in fatigue ~1.3 to 1.5 cm beyond the mechanical notch to produce a sharp, natural crack. The compliance of each cracked specimen (load to produce a given displacement) was then experimentally determined in order to calibrate each specimen prior to the application of the test loads. Displacements were measured with a clip gage constructed to the requirements of ASTM E399 [6]. Theoretical displacements were calculated using the relationship of Saxena and Hudak [7] to verify that the load-displacement relationships were as predicted. Excellent agreement was noted between theoretical and measured compliances. The specimen compliance calibration was used to achieve the desired initial K-level (stress-intensity level) when loading the specimen prior to testing.

TABLE II

Composition of Materials in Slow Strain Rate Tests.

Element	wt%	Element	wt%
AISI 1020 Steel			
C	0.20	P	0.025
Mn	0.56	S	0.026
ASTM A27 (Grade 60-30) Steel (Heat #2155382)			
C	0.245	P	0.016
Mn	0.69	S	0.018
Si	0.59		
ASTM A387 (Grade 9) Steel (Heat #46625)			
C	0.10	Si	0.29
Mn	0.48	Cr	8.36
P	0.010	Mo	0.96
S	0.011		
90-10 Cupronickel (CDA 706, Hussey Metal Div. Lot 971)			
Cu	88.76	Ni	9.8
Fe	1.05	Mn	0.20
Zn	0.17	C	0.007-0.011
P	0.005	S	0.004
OFHC Copper (CDA 102, Hitachi Cable #91E0395)			
Cu	99.99	P	0.002
Bi	<0.001	Se	<0.001
Cd	<0.001	S	0.013
Pb	0.004	Te	<0.001
Hg	<0.001	Zn	<0.001
O_2	0.003		

During static-load testing, the specimens were loaded to the desired K value by torquing the loading bolt until the desired value of crack mouth opening displacement (from the known compliance relationship) was achieved. To ensure that all deformation and any crack formation occurred in the presence of groundwater, strips of plastic tape were employed on both specimen faces, and the notch and crack area were filled with groundwater during loading. Test specimens (with tape removed) were

TABLE III

Composition of Synthetic Grande Ronde 2 (GR-2) Groundwater Solution.

Element	mg/L	Element	mg/L
Na^+	250	OH^-	1.4
K^+	1.9	$H_3SiO_4^-$	103
Ca^{+2}	1.3	Cl^-	148
Mg^{+2}	0.40	SO_4^{-2}	108
CO_3^{-2}	27	F^-	37
HCO_3^-	70	pH	9.9

then placed in an autoclave partially filled with groundwater. The autoclave was then filled with groundwater, crushed basalt, and bentonite packing material, and brought to the desired 100 atmospheres (10.1 MPa) of pressure and desired test temperature. The pressure simulated hydrostatic pressure at the repository depth. Test temperatures were 150 and 250 °C. The autoclave contents were essentially static during testing.

Specimens were removed from the autoclaves after the desired exposure, and posttest compliance measurements were taken. The specimens were immersed in liquid nitrogen to embrittle them. Then the specimens were fractured along the line of the existing crack. Optical measurements of the crack length and examination of the crack surfaces were performed. Comparisons of pre- and posttest compliance and crack examination results were used to determine if any extension of the crack occurred during the test.

Cyclic loading specimens were tested according to American Society for Testing and Materials (ASTM) Standard E647 [8] in servo-hydraulic machines operated in load-control mode. Loads were controlled to within 1% or less. Sinusoidal wave forms with stress ratios (minimum load/maximum load) of 0.05 were used for all tests. Cyclic frequencies ranged from 0.1 to 10 Hz. The test environments were air, vacuum, and simulated basalt groundwater, with test temperatures of 150 and 250 °C. Tests in groundwater were conducted at 68 atmospheres (6.9 MPa) of pressure in low-flow autoclaves [9].

Material compositions are given in Table IV. The A36 steel was in the form of hot-rolled plate; the A387-9 steel plate was normalized at 899 °C for 60 min and furnace cooled, then annealed at 704 °C for 250 min and air cooled. The A27 material was cast and was from the same heat of material as given in Table II. The room temperature 0.2% yield strength of the A36 material was 316 MPa while the room temperature ultimate strength was 468 MPa. The A387 steel had a room temperature 0.2% yield strength of 523 MPa and a room temperature ultimate strength of 686 MPa.

The groundwater compositions used in the fracture mechanics tests were the Grande Ronde 4 composition shown in Table I for cyclic loading tests and the "Equilibrium Groundwater" composition shown in Table V for static loading tests. Current tests employ the Grande Ronde 4 groundwater. Little difference in effects of the differing compositions is expected.

TABLE IV

Composition of Materials in Fracture Mechanics Tests.

Element	Wt%	Element	Wt%
ASTM A36 Steel (Heat Y45659)			
C	0.15	P	0.23
Si	0.2	S	0.014
Mn	0.96	Cu	0.02
ASTM A387 (Grade 9) Steel (Heat 45862)			
C	0.11	S	0.013
Si	0.23	Mo	0.94
Mn	0.59	Cr	8.70
P	0.012		

TABLE V

Equilibrium Groundwater Composition.

Element	mg/L	Element	mg/L
Na^+	518	Cl^-	287
K^+	55	SO_4^{-2}	365
Ca^{+2}	10.8	HCO_3^-	482
Si	205	pH	8.1
F-	16.5		

RESULTS AND DISCUSSION

Slow Strain Rate

Results of the slow strain-rate tests are given in Table VI and Fig. 3 through 7. Yield and ultimate strength values are omitted for clarity as they were identical in air and groundwater environments and effects on ductility were the principal focus of the investigations. Some of the results below were reported in BWIP reports SD-BWI-TI-152 [10] and SD-BWI-TS-008 [11].

The tests of 1020 wrought steel showed minor effects of orientation with the specimens strained perpendicularly to the rolling direction having the least ductility in both air and groundwater. The tests in groundwater had much lower reduction of area values at the slowest strain rate and showed areas of intergranular fracture, indicating effects of EAC.

The results for the A27 cast carbon steel show less ductility in general than the 1020 steel and less effects of groundwater on ductility reduction. Two of the A27 tests employed test environment differences felt to better represent the anoxic groundwater expected to be found in the candidate horizon, the Cohassett flow. These differences were the Grande Ronde 4 groundwater chemistry and argon sparging rather than argon/20% oxygen. No significant effect of the changes was apparent from the test results. Some minor surface cracking of the A27 specimens was noted, but the fracture surfaces all exhibited ductile microvoid coalescence.

Test results for the A387 (Grade 9) steel displayed significant reduction in ductility at the slower strain rates. Evidence of EAC was noted on fracture surfaces of the A387 specimens.

TABLE VI

Results of Slow Strain-Rate Tests on BWIP Candidate Containers. (sheet 1 of 2)

Specimen	Orientation[a]	Strain rate(s)	Elongation (%)	Reduction of area (%)
1020 Carbon Steel (Wrought), Test Temperature 150 °C, (Environment, Air)				
N394	TL	1×10^{-4}	21.0	56.9
N395	TL	1×10^{-4}	21.5	51.5
N412	LT	1×10^{-4}	24.0	62.9
N413	LT	1×10^{-4}	24.7	60.8
N410	LT	2×10^{-7}	26.7	60.2
N415	LT	2×10^{-7}	27.5	61.0
1020 Carbon Steel (Wrought), Test Temperature 150 °C, (Environment, Grande Ronde 2)				
N403	TL	1×10^{-4}	22.6	59.5
N404	TL	1×10^{-4}	21.5	54.6
N420	LT	1×10^{-4}	25.1	62.2
N421	LT	1×10^{-4}	24.0	63.8
N407	TL	2×10^{-7}	16.7	19.4
N396	TL	2×10^{-7}	20.0	35.3
N416	LT	2×10^{-7}	22.8	45.7
A27 (Grade 60-30) Carbon Steel (Cast), Test Temperature 150 °C, (Environment, Air)				
P473	--	1×10^{-4}	17.8	24.3
P475	--	1×10^{-4}	20.0	39.4
P472	--	2×10^{-7}	17.6	19.7
P467	--	2×10^{-7}	18.0	27.1
A27 (Grade 60-30) Carbon Steel (Cast), Test Temperature 150 °C, (Environment, Grande Ronde 4)				
P469	--	1×10^{-4}	18.6	29.6
A27 (Grade 60-30) Carbon Steel (Cast), Test Temperature 150 °C, (Environment, Grande Ronde 2)				
P471	--	1×10^{-4}	19.7	26.1
P468	--	2×10^{-7}	13.0	16.4
P470	--	2×10^{-7}	13.0	14.5
P474[b]	--	2×10^{-7}	10.0	12.9
A387 (Grade 9) Alloy Steel (Tempered Plate), Test Temperature 150 °C, (Environment, Air)				
P499	--	1×10^{-4}	21.0	63.5
P514	--	2×10^{-7}	20.0	63.8
A387 (Grade 9) Alloy Steel (Tempered Plate), Test Temperature 150 °C, (Environment, Grande Ronde 4)				
P502	--	1×10^{-4}	21.0	64.5
A387 (Grade 9) Alloy Steel (Tempered Plate), Test Temperature 150 °C, (Environment, Grande Ronde 2)				
P511	--	1×10^{-4}	20.0	66.8
P501	--	1×10^{-4}	20.0	62.2
P507	--	1×10^{-4}	20.0	64.5
P497	--	1×10^{-6}	16.0	24.9
P500	--	1×10^{-6}	18.0	40.1
P509	--	2×10^{-7}	(c)	23.1
P510	--	2×10^{-7}	6.0	21.5
P498[b]	--	2×10^{-7}	(c)	16.8
P506b	--	2×10^{-7}	(c)	22.0

TABLE VI

Results of Slow Strain-Rate Tests on BWIP Candidate Containers. (sheet 2 of 2)

Specimen	Orientation[a]	Strain rate(s)	Elongation (%)	Reduction of area (%)
90-10 Cupronickel (Annealed), Test Temperature 100 °C, (Environment, Air)				
Q696	--	1×10^{-4}	44	55
Q690	--	2×10^{-7}	40	67
Q693	--	2×10^{-7}	37	64
90-10 Cupronickel (Annealed), Test Temperature 100 °C, (Environment, Grande Ronde 4)				
Q689	--	1×10^{-4}	43	66
Q697	--	1×10^{-4}	40	67
Q691	--	2×10^{-7}	40	62
Q694	--	2×10^{-7}	38	62
90-10 Cupronickel (Annealed), Test Temperature 200 °C, (Environment, Air)				
Q700	--	1×10^{-4}	38	60
R608	--	1×10^{-4}	46	63
Q695	--	2×10^{-7}	33	46
R613	--	2×10^{-7}	39	60
90-10 Cupronickel (Annealed), Test Temperature 200 °C, (Environment, Grande Ronde 4)				
R611	--	1×10^{-4}	44	61
R612	--	1×10^{-4}	42	66
Q610	--	2×10^{-7}	38	46
OFHC Copper (Wrought), Test Temperature 100 °C, (Environment, Air)				
R466	--	1×10^{-4}	15	31
R467	--	2×10^{-7}	5	2
OFHC Copper (Wrought), Test Temperature 100 °C, (Environment, Grande Ronde 4)				
R468	--	1×10^{-4}	15	23
R465	--	1×10^{-4}	10	23
R472	--	2×10^{-7}	5	4
R474	--	2×10^{-7}	4	3
OFHC Copper (Wrought), Test Temperature 200 °C, (Environment, Air)				
R475	--	1×10^{-4}	4	6
R476	--	1×10^{-4}	6	4
R473	--	2×10^{-7}	1	3
R477	--	2×10^{-7}	3	1
OFHC Copper (Wrought), Test Temperature 200 °C, (Environment, Grande Ronde 4)				
R479	--	1×10^{-4}	5	6
R480	--	1×10^{-4}	7	6
R482	--	2×10^{-7}	3	1

[a]LT = Stressed parallel to plate rolling direction, TL = stressed perpendicular to plate rolling direction.

[b]Argon-sparged groundwater; other tests employed Argon/20% O_2.

[c]Gage marks were removed to avoid fracture initiation, so elongation data are not available.

The tests of 90-10 Cupronickel showed little effects of groundwater environment or strain rate on ductility.

The OFHC copper specimen ductility displayed severe temperature and strain-rate dependence. No effects of the groundwater environment were apparent. The lack of ductility at high temperatures and low strain rates resulted from a change in the fracture mode of copper from transgranular to intergranular.

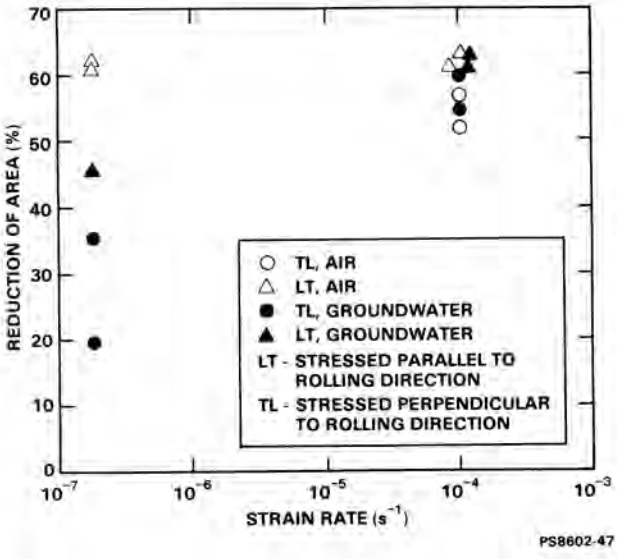

Fig. 3. Slow Strain Rate Results for 1020 Wrought Carbon Steel (150 °C).

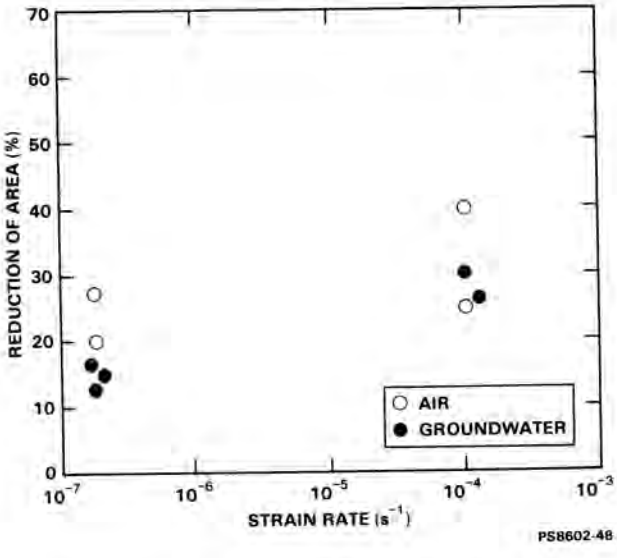

Fig. 4. Slow Strain Rate Results for A27 Case Carbon Steel (150 °C).

The results of copper alloy tests are consistent with results of other investigators (See References 12, 13, 14).

Fracture Mechanics

Results from fracture mechanics tests are given below. Some results of tests have appeared in BWIP reports SD-BWI-TI-165 [15] and SD-BWI-TS-012 [16].

Parameters of static load tests on A36 carbon steel wrought plate and A387 (Grade 9) low-alloy steel are given in Table VII. The objective of these tests is to determine if the fatigue cracks within the specimens will grow from environmental effects during the test. Examination of posttest crack surfaces and comparison of final crack length with initial crack length (predicted from compliance

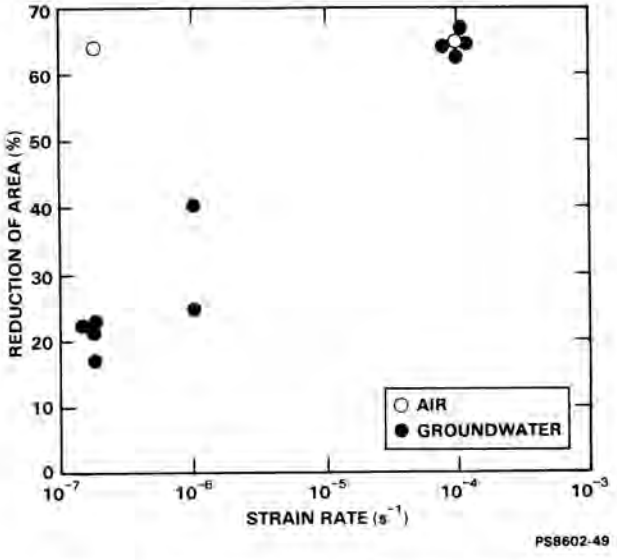

Fig. 5. Slow Strain Rate Results for A387 Low-Alloy Steel (150 °C).

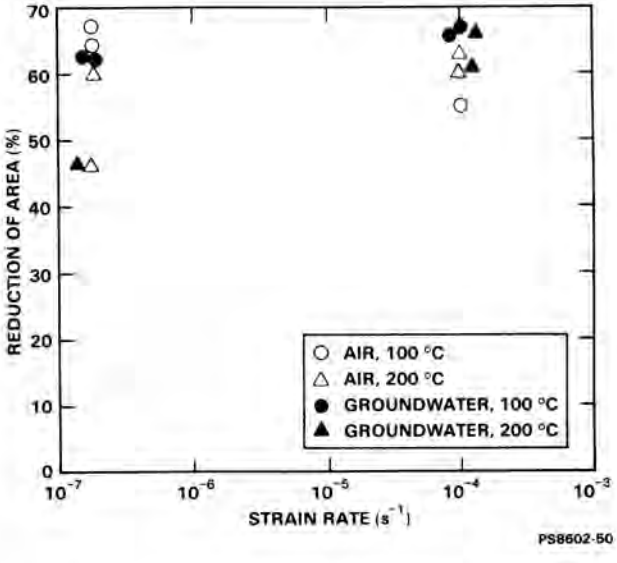

Fig. 6. Slow Strain Rate Results for 90-10 Cupronickel (100 and 200 °C).

measurements) showed no extension for any of the A36 specimens. The A387 specimen with the highest stress may have had limited crack extension, but results were not conclusive.

Results of cyclic load tests on A36 wrought carbon steel, A27 cast carbon steel, and A387 low-alloy steel are given in Fig. 8 through 10. No tabular data are presented as they would not be informative. Tests at 250 °C are given in Fig. 8, for A36 and A27 steel. Limited results in

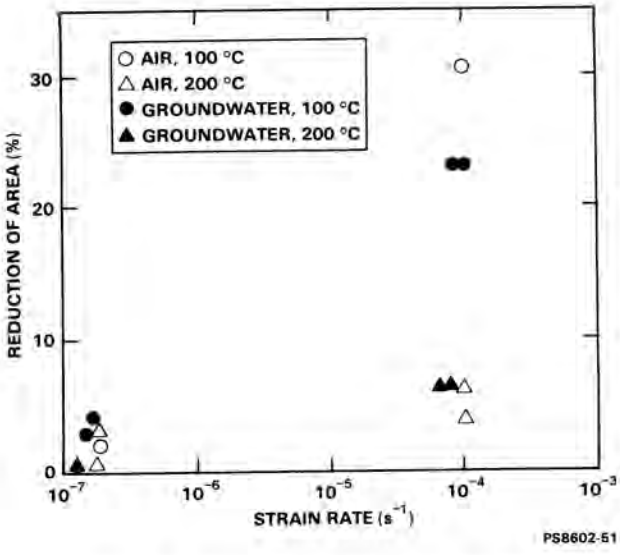

Fig. 7. Slow Strain Rate Results for Oxygen-Free High-Conductivity Copper (100 and 200 °C).

TABLE VII

Static Load Test Conditions

Specimen No.	Alloy	Precrack Max. K, MPa $\sqrt{m}$	Initial test K, MPa $\sqrt{m}$
Test 1 with Exposure Conditions (<24 h at 250 to 270 °C)			
2681	A36	22.7	30.1
2680	A36	22.9	40.5
2682	A36	26.2	60.2
2698	A387-9	23.1	30.2
2699	A387-9	24.0	40.2
2700	A387-9	25.8	60.2
Test 2 with Exposure Conditions (2,180 h at 150 °C)			
2683	A36	23.4	30.4
2686	A36	28.1	40.0
2687	A36	39.8	60.1
2705	A387-9	24.2	30.3
2704	A387-9	25.6	40.1
2702	A387-9	27.8	60.1
Test 3 with Exposure Conditions (2,000 h at 250 °C)			
2685	A36	25.4	30.9
2689	A36	23.3	40.4
2684	A36	24.0	60.3
2701	A387-9	24.0	30.1
2706	A387-9	24.7	40.3
2707	A387-9	28.4	60.0

K = Stress intensity factor.

groundwater show behavior midway between that found in air and vacuum reference environments; in other words, no enhancement of fatigue crack growth by the groundwater was observed. No effects of cyclic frequency were noted, but data with differing

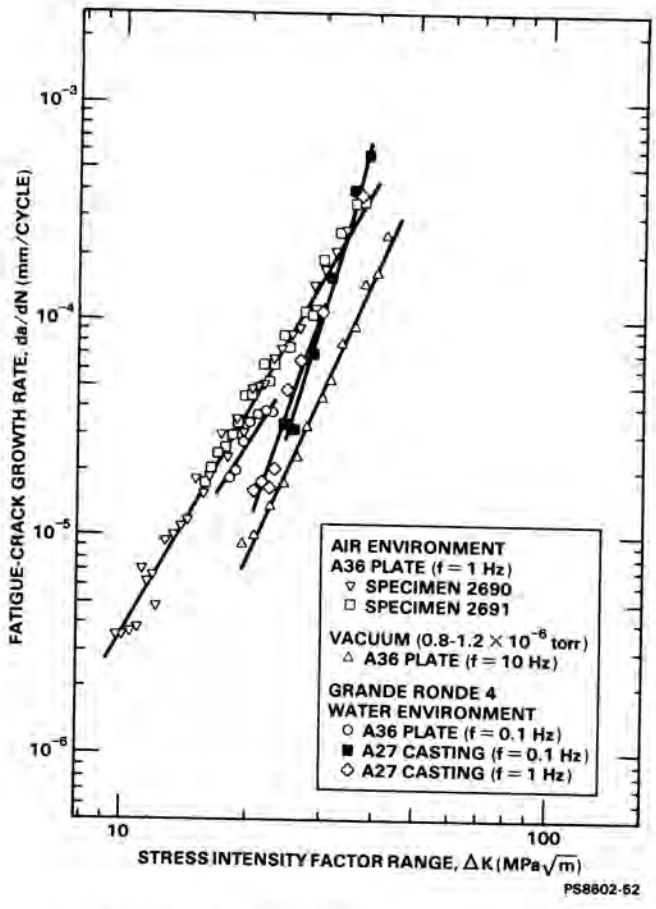

Fig. 8. Fatigue Crack Propagation in Carbon Steels at 250 °C.

frequencies are limited. Similar results are given in Fig. 9 for tests at 150 °C. Results for the A387 steel in air and vacuum are given in Fig. 10. No data for specimens in groundwater were available.

CONCLUSIONS

The slow strain-rate tests showed a variety of responses to testing in air and groundwater. The 90-10 Cupronickel specimens had no change in ductility with test environment. The OFHC copper data displayed significant decreases in ductility with increasing temperature and decreasing strain rate but no change with the test environment. The carbon steel data showed decreases in ductility and tendencies for brittle fracture, evidence of EAC. The A387 steel had the greatest susceptibility for EAC the A27 steel had minor effects of EAC.

The cyclic load tests are just beginning. Results to date exhibit no effect of groundwater on crack growth rates, and little effect of frequency. Low-frequency tests are important as they are closer to the prototypic case of static loading that will be felt by the actual waste container. However, the experimental time to achieve the broad range of crack growth rates desired is greater with low frequencies.

The slow strain-rate tests are nearly complete on the base candidate container materials.

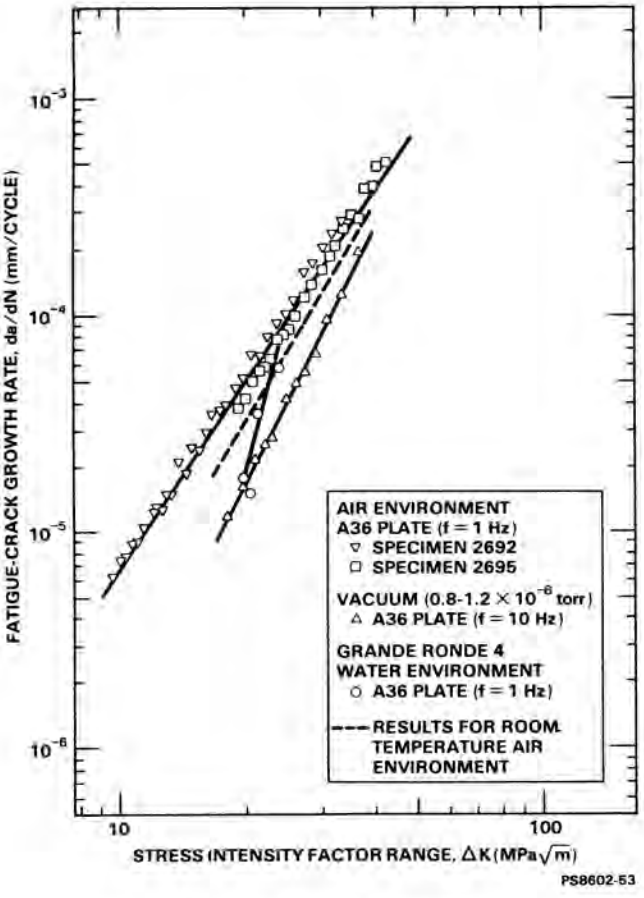

Fig. 9. Fatigue Crack Propagation in A36 Steel at 150 °C.

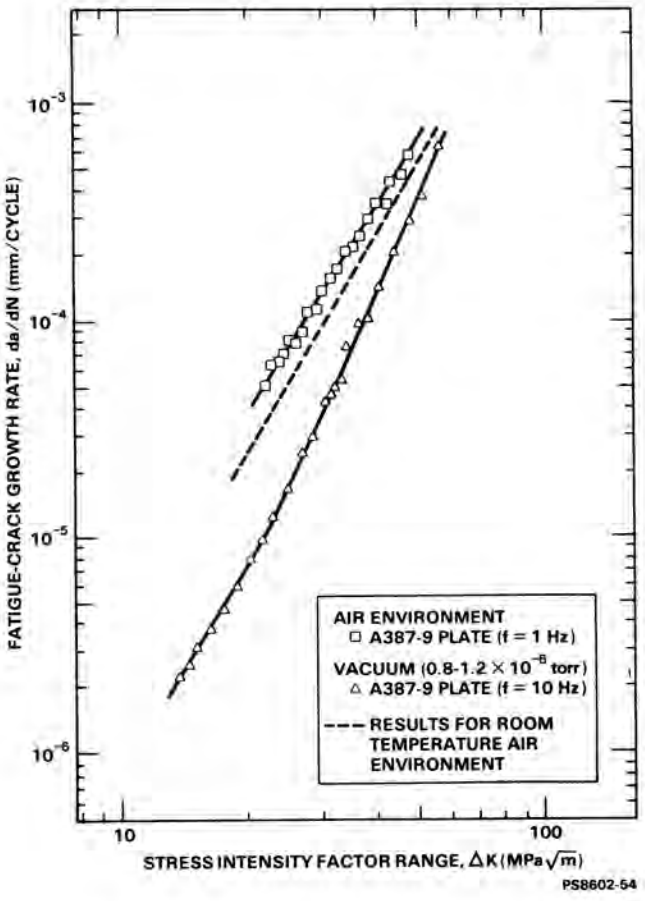

Fig. 10. Fatigue Crack Propagation in A387 Steel at 250 °C.

Additional tests to investigate intermediate strain rates and investigate effects of annealing (to simulate the cast form expected in actual containers) on OFHC copper properties will be completed in 1986. Future tests will focus on weld material properties.

The fracture mechanics testing in the future will complete the testing on the A27 carbon steel in groundwater with several cyclic frequencies and temperatures from 50 to 250 °C. The crack growth data will be extrapolated to very low rates to obtain a conservative threshold stress for EAC. Testing on the A387 steel has been minimized in comparison to the A27 steel because of the greater susceptibility to EAC shown by A387 steel in slow strain-rate tests. Testing on OFHC copper and 90-10 Cupronickel is beginning with determinations of load relaxation, which will be significant for copper materials at repository temperatures. Major relaxation of loads would remove a necessary driving force for EAC and render it impossible. Investigations of load relaxation will be complete in 1986.

To summarize, the slow strain-rate tests have given a ranking of EAC susceptibility of the BWIP candidate container alloys from least for both copper alloys to greatest for the low-alloy steel. These results will be useful in future alloy-selection efforts and to corroborate findings with fracture mechanics tests. The fracture mechanics results have shown no conclusive crack extension in static load tests, an encouraging result in relation to container integrity. The absence of groundwater enhancement of fatigue crack growth, if it continues, is also positive with respect to demonstration of container integrity.

REFERENCES

1. NRC (U.S. Nuclear Regulatory Commission), Disposal of Nuclear Radioactive Waste in Geological Repositories; Final Rules, Title 10, Code of Federal Regulations, Part 60, Washington, D.C., 1985.

2. Lane, D. L., T. E. Jones, and M. H. West, "Preliminary Assessment of Oxygen Consumption and Redox Conditions in a Nuclear Waste Repository in Basalt," Geochemical Behavior of Disposed Radioactive Waste, American Chemical Society Symposium Series #246, American Chemical Society, Washington, D.C., 1984, p. 181.

3. National Materials Advisory Board, Characteristics of Environmentally Assisted Cracking for Design, Report NMAB-386, National Academy of Sciences, Washington, D.C., 1982.

4. James, L. A. and L. D. Blackburn, Basalt Waste Isolation Project Crack Growth Studies, SD-BWI-TI-120, Rockwell Hanford Operations, Richland, Washington, 1984.

5. Novak, S. R. and S. T. Rolfe, "Modified WOL Specimen for K_{ISCC} Environmental Testing," Journal of Materials, vol. 4, no. 3, pp. 701-728, 1969.

6. ASTM (American Society for Testing and Materials), "Standard Test Method for Plane-Strain Fracture Toughness of Metallic Materials," E 399-83, 1985 Annual Book of ASTM Standards, vol. 03.01, pp. 547-582, Philadelphia, Pennsylvania, 1983.

7. Saxena, A. and S. J. Hudak, "Review and Extension of Compliance Information of Common Crack Growth Specimens," International Journal of Fracture, vol. 14, no. 5, pp. 453-468, 1978.

8. ASTM (American Society for Testing and Materials), "Standard Test Method for Constant Load Amplitude Fatigue Crack Growth Rates Above 10^{-8} m/cycle," E 647-83, 1985 Annual Book of ASTM Standards, vol. 03.01, pp. 739-759, Philadelphia, Pennsylvania, 1985.

9. James, L. A. and L. J. Ceschini, "A New Method for In Situ Compliance Measurements for Fatigue Crack Growth Testing in Autoclaves," Journal of Testing and Evaluation, vol. 13, no. 6, pp. 409-415, 1985.

10. Pitman, S. G., Enviromechanical Testing of AISI 1020 Steel in Hanford Grande Ronde Groundwater, SD-BWI-TI-152, Rockwell Hanford Operations, Richland, Washington, 1983.

11. Pitman, S. G., Slow-Strain-Rate Testing of 9%Cr, 1%Mo Wrought Steel and ASTM A27 Cast Steel in Hanford Grande Ronde Groundwater, SD-BWI-TS-008, Rockwell Hanford Operations, Richland, Washington, 1985.

12. Greenwood, J. N., D. R. Miller, and J. W. Suiter, "Intergranular Cavitation in Stressed Metals," Acta Metallurgia, Vol. 2, p. 250, 1954.

13. Reid, B. J. and J. N. Greenwood, "Intergranular Cavitation in Stressed Copper-Nickel Alloys," Transactions of the Metallurgical Society of AIME, p. 503, August 1958.

14. Chen, C. W and E. S. Machlin, "The Effect of Grain Boundary Migration on the Formation of Intercrystalline Voids During Creep," Transactions of the Metallurgical Society of AIME, p. 177, vol. 218, 1960.

15. James, L. A. and L. D. Blackburn, Technical Progress Report on BWIP Canister Materials Crack Growth Study for FY 1983, SD-BWI-TI-165, Rockwell Hanford Operations, Richland, Washington, 1984.

16. James, L. A., Short-Term Stress-Corrosion-Cracking Tests for A36 and A387-9 Steels in Simulated Hanford Groundwater, SD-BWI-TS-012, Rockwell Hanford Operations, Richland, Washington, 1985.